1 **Chemical ionization of clusters formed from sulfuric acid and dimethylamine or diamines**

2 Coty N. Jen[1,2*], Jun Zhao[1,3], Peter H. McMurry[1], David R. Hanson[4]

3 [1]Department of Mechanical Engineering, University of Minnesota – Twin Cities, 111 Church St. SE,
4 Minneapolis, MN, 55455, USA
5 [2] now at Department of Environmental Science, Policy, and Management, University of California,
6 Berkeley, Hilgard Hall, Berkeley, CA, 94720
7 [3] now at Institute of Earth Climate and Environment System, Sun Yat-sen University, 135 West Xingang
8 Road, Guangzhou 510275, China
9 [4]Department of Chemistry, Augsburg College, 2211 Riverside Ave., Minneapolis, MN, 55454, USA
10
11 *corresponding author email: jenco@berkeley.edu
12

13 **Supporting Information:**

19 **S1.   Mass-dependent sensitivity of the Cluster CIMS:**

20   Mass-dependent sensitivity experiments were performed on the University of MN Cluster
21 CIMS following a near identical procedure as detailed in Zhao et al. (2010), with pertinent
22 details described here. Four tetra-alkyl ammonium halide salts were used in this experiment:
23 tetramethyl ammonium iodide (TMAI at 74 and 275 amu), tetrapropyl ammonium iodide (TPAI
24 at 186 amu), tetrabutyl ammonium iodide (TBAI at 242 amu), and tetraheptyl ammonium
25 bromide (THAB at 410 amu). These salts were dissolved in methanol and electrosprayed in
26 positive ion mode. Specific ion mobilities (Ude and de la Mora, 2005) were selected using a high
27 resolution differential mobility analyzer (HDMA) (Rosser and de la Mora, 2005). The flow
28 containing mono-mobile ions was split into two equal streams with one measured by an
29 electrometer and the other by the Cluster CIMS. The ions were directly delivered to the inlet of
30 the Cluster CIMS where they first entered a conical octopole (1 MHz and 24 V pk-pk) then the
31 quadrupole mass analyzer. The signals of the Cluster CIMS were then divided by the
32 electrometer measured concentrations to obtain the sensitivity. Since the ions were delivered
33 directly to the Cluster CIMS inlet, these experiments only probe the mass-dependent sensitivity
34 of the inlet, octopole, quadrupole, and detector.
35   Figure S1 shows measured sensitivity at specific masses corresponding to the alkyl halide
36 positive ions (black squares). We assume the mass-dependent sensitivity for positive ions is the
37 same for negative ions. The sensitivity at smaller masses is lower than at larger masses,
38 indicating that the Cluster CIMS more efficiently measures larger ions. For masses between 410
39 to 710 amu, we assume a sensitivity value of 0.037 Hz cm^3 (green line). Masses larger than 710
40 amu are not detected (i.e., sensitivity of zero) due to limits of our quadrupole. A constant
41 sensitivity assumes that all mass from ~200-710 amu are measured with equal efficiency. This

42 contrasts with Zhao et al. (2010) where they observed a steep decline in sensitivity at large
43 masses. We based our assumption on the size and shape of largest mass peaks. Figure S2 shows
44 a sample mass scan of sulfuric acid with [EDA]=60 pptv. The largest ion detected is $A_6^- \cdot EDA_2$ at
45 707 amu. The peak is ~4 amu wide and ~600 Hz tall. If the sensitivity for this large ion were
46 low, then the resulting $[A_6^- \cdot EDA_2]$ would exceed that of $[A_2^-]$, an unlikely scenario.
47   The uncertainties associated with the sensitivity depend on the ion masses being
48 compared. For ions similar in mass, such as $HNO_3 \cdot NO_3^-$ (125 amu) and $HNO_3 \cdot HSO_4^-$ (160 amu),
49 the uncertainty is small at ~20%. However, taking the ratio between various sulfuric acid clusters
50 and the acetate reagent ion signals can result in uncertainties up to a factor of 2 to 3. This large
51 uncertainty is due to extrapolating between the two smallest ion masses studied in the sensitivity
52 measurements: 74 to 186 amu. In addition, the acetate reagent ions are all very small and fall on
53 the steep rise of the sensitivity curve. More sensitivity experiments are required in the low mass
54 range to reduce this uncertainty.

55
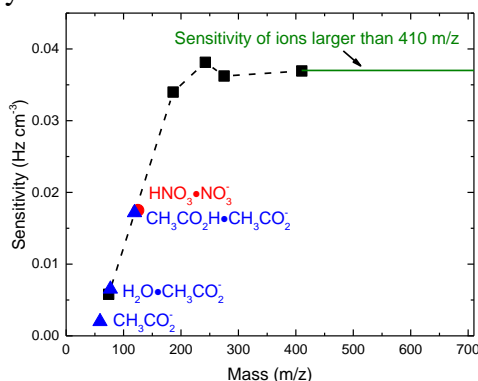
56 **Figure S1 Sensitivity of the UMN Cluster CIMS as a function of mass. The black squares indicate the measured sensitivity**
57 **of the positive alkyl halide ions. The blue triangles show the predicted sensitive of the acetate ions with three different**
58 **ligands. The red circle is the sensitivity of the nitrate dimer ion. The dark green line is the extrapolated sensitivity for**
59 **masses larger than 410 amu.**

60
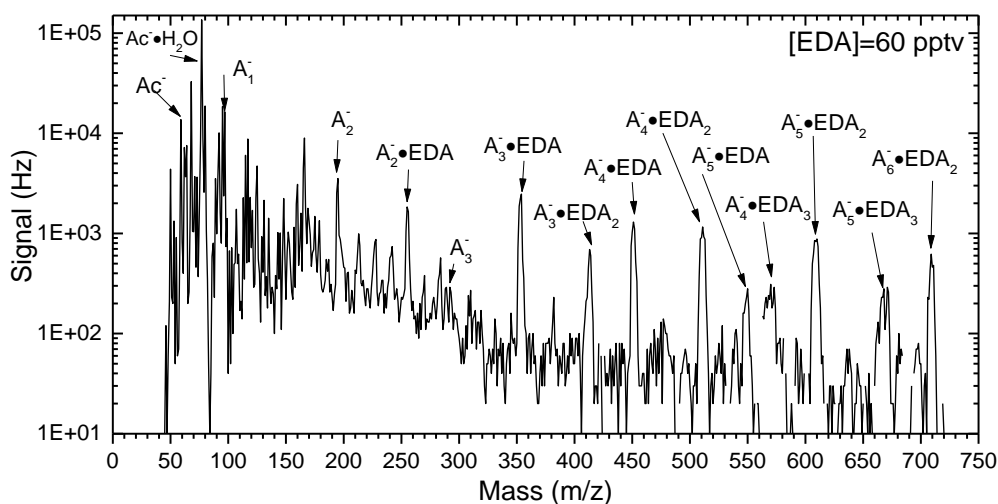
61 **Figure S2 Mass scan of sulfuric acid at $[A_1]_0=4 \times 10^9$ cm^{-3} and [EDA]=60 pptv measured using acetate (Ac$^-$). Identities of**
62 **sulfuric acid+EDA peaks are labeled.**

S2. Nitrate vs. acetate mass spectra comparison for sulfuric acid+diamine

Figure S3 compares nitrate and acetate mass spectra for the three diamines at equivalent $[A_1]_o$ and $[B]$. As no other parameters of the Cluster CIMS changed between nitrate and acetate measurements, Figure S3 clearly shows that nitrate does not chemically ionize all types of sulfuric clusters in the presence of diamines. It is possible that larger ion clusters decompose to a greater extent with acetate CI than nitrate and lead to increased signal for the clusters shown in Figure S3. However, normalized acetate signals are 10 times larger than nitrate signals which would require very high and nonsensical concentrations of the larger clusters for decomposition to be the sole reason for the difference. Furthermore, nitrate detects small amounts of A_3^- •diamine; this could be due to decomposition of larger ions, IIC from $N_2+A_1^-$, or partially efficient nitrate CI of A_3•diamine.
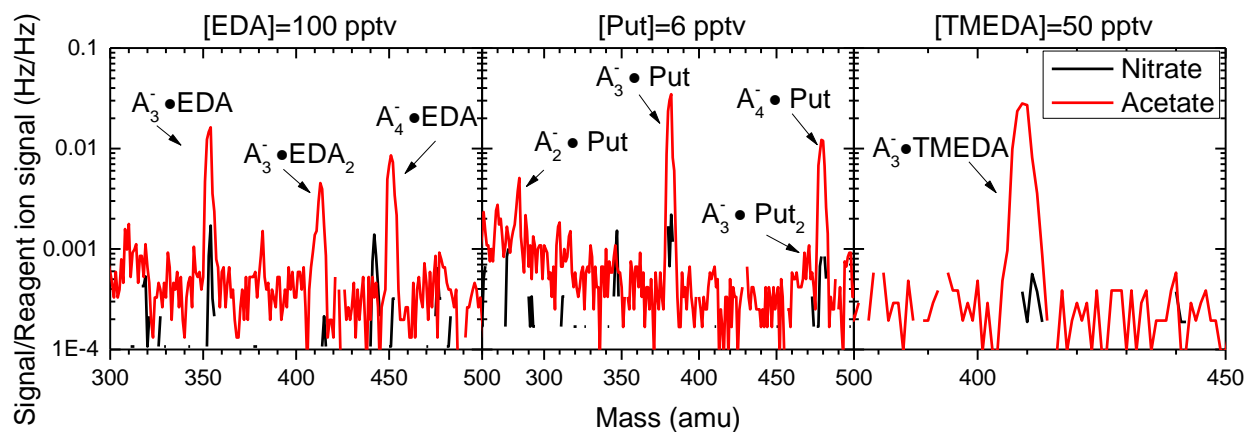
Figure S3 Comparison between nitrate (black) and acetate (red) mass spectra for EDA (left), Put (center), and TMEDA (right). The concentration of diamine for the comparison is given at the top of each panel.

S3. $[N_1]$ and $[N_2]$ from mass spectrometer signals

The depletion of the reagent ion (given here as $[NO_3^-]$) can be written as

$$\frac{d\left[NO_3^-\right]}{dt_{CI}} = -k_1\left[N_1\right]\left[NO_3^-\right]$$

Equation S1

This assumes that the reagent ion only reacts with N_1. This has a solution of

$$\left[NO_3^-\right] = \left[NO_3^-\right]_o \exp\left(-k_1\left[N_1\right]t_{CI}\right)$$

Equation S2

Assuming $[A_1^-]$ is not formed in appreciable quantities by ion fragmentation, then the formation of $[A_1^-]$ can be written as

$$\frac{d\left[A_1^-\right]}{dt_{CI}} = k_1\left[N_1\right]\left[NO_3^-\right] - k_{21}\left[A_1^-\right]\left[N_1\right]$$

Equation S3

85

86 Substituting Equation S2 into Equation S3 gives

$$\frac{d\left[A_1^-\right]}{dt_{CI}} = k_1\left[N_1\right]\left[NO_3^-\right]_o \exp\left(-k_1\left[N_1\right]t_{CI}\right) - k_{21}\left[A_1^-\right]\left[N_1\right]$$

Equation S4

87

88 Where $[NO_3^-]_o$ is the initial concentration of NO_3^-. Equation S4 can be solved to give

89

$$\left[A_1^-\right] = k_1\left[NO_3^-\right]_o\left(\frac{\exp\left(-k_1\left[N_1\right]t_{CI}\right) - \exp\left(-k_{21}\left[N_1\right]t_{CI}\right)}{k_{21} - k_1}\right)$$

Equation S5

90 Equation S2 can be inserted in Equation S5 to remove $[NO_3^-]_o$.

$$\frac{\left[A_1^-\right]}{\left[NO_3^-\right]} = \frac{S_{160}}{S_{125}} = \frac{k_1}{k_{21} - k_1}\left(1 - \exp\left(\left(k_1 - k_{21}\right)\left[N_1\right]t_{CI}\right)\right)$$

Equation S6

91 The signal at the ion's mass directly relates to the ion concentration (plus a mass-
92 dependent sensitivity that we do not include in this derivation for simplicity but is included in the
93 model); therefore, the $[A_1^-]$ can be replaced by S_{160} (bisulfate with a nitric acid ligand with a total
94 mass of 160 amu) and $[NO_3^-]$ with S_{125} (nitrate with a nitric acid ligand for a mass of 125 amu).
95 Equation S6 is a more accurate method to convert signal ratios to neutral concentration then the
96 equations given in Berresheim et al. (2000) and Eisele and Hanson (2000) as this equation does
97 not assume constant concentrations of the reagent ion. However, at very short t_{CI} (like the 15 to
98 18 ms used here), Equation S6 results in $[N_1]$ about 5% higher than using the logarithmic
99 equation given in Berresheim et al. (2000) and 1% higher than the simple ratio equation of Eisele
100 and Hanson (2000).

101 The derivation for $[A_2^-]$ (S_{195}) follows similar math as for $[A_1^-]$. The relation for $[A_2^-]$ as a
102 function of t_{CI} is given in Equation S7 and can be divided by Equation S5 to obtain S_{195}/S_{160} vs.
103 t_{CI} (not shown).

$$\left[A_2^-\right] = \frac{k_{21}k_1}{k_{21} - k_1}\left[NO_3^-\right]_o \left\{\begin{array}{l} \exp\left(-k_1\left[N_1\right]t_{CI}\right)/\left(k_{32} - k_1\right) + \exp\left(-k_{21}\left[N_1\right]t_{CI}\right)/\left(k_{21} - k_{32}\right) \\ -\exp\left(-k_{32}\left[N_1\right]t_{CI}\left(k_{21} - k_1\right)\right)/\left(\left(k_{32} - k_1\right)\left(k_{21} - k_{32}\right)\right) \end{array}\right\}$$

Equation S7

104 Ratio of cluster signals to the reagent ion can be affected by several factors not
105 considered in Equation S6. 1) Varying relative humidity alters the number of water ligands
106 attached to charged and neutral clusters. This will alter the kinetics and stability of clusters, thus
107 changing the amount and types of clusters detected. 2) The addition of base into the flow reactor
108 introduces a small stream of nitrogen that may locally dilute $[N_1]$ by up to 40% with very high
109 base addition flow rates prior to Cluster CIMS measurement. 3) Very high concentration of
110 nitrate ion will allow more mixed clusters to be detected, i.e. $A_m^- \cdot B_j \cdot HNO_3$. Our measurements
111 indicate that the stability of these clusters also depends on RH. 4) Prior to entering into the

112 vacuum region of the Cluster CIMS, the ions pass through a curtain gas flow consisting of 200
113 sccm of nitrogen. This flow slightly exceeds the flow into the mass spectrometer and may might
114 cause ion clusters to evaporate. More information on cluster chemistry can be gained by studying
115 how these factors alter observed clusters and their concentrations.
116
117 **S4.   Modeled reactions and parameters**
118   The modeled reactions can be divided into three categories: neutral cluster formation,
119 chemical ionization and ion decomposition, and IIC. Table S2 lists all the reactions that were
120 modeled. The neutral cluster forward rate constants, k, were assumed to be $4x10^{-10}$ cm^3 s^{-1}, and
121 the ion forward rate constants, k_c, were taken to be $2x10^{-9}$ cm^3 s^{-1}. Some error is introduced in
122 these forward rate constants but is likely small compared to other sources of uncertainty such as
123 evaporation or decomposition rates. To constrain the number of parameters, we assumed ions
124 either instantly decompose or do not decompose at all. Decomposition rate constants listed as
125 *fast* were assumed to be instantaneous and the intermediate products do not form in appreciable
126 quantities. Ion decomposition rate constants listed as $E_{A_iB_j^-}$ were assumed to be zero.

127   Table S1 provides the neutral cluster evaporation rates used for the model that produced
128 good agreement with our observations. We examined numerous sets of neutral and ion
129 evaporation rate combinations to determine if our measured signal ratios as a function of CI
130 reaction time for the diamines could be explained by simple changes in evaporation rates.
131 However, no sensible combination reproduced our observations, leading us to believe that some
132 fraction of [N$_2$] with diamines is not chemically ionized by nitrate.
133   These evaporation rates are by no means the "correct" rates. Our model only considered
134 clusters up to size 4. The dynamics of the larger clusters likely effect the apparent evaporate rates
135 of the smaller clusters. The evaporation rates also indicate that the clusters have lifetimes on the
136 order of neutral reaction time of 3 s. Therefore, we cannot say with confidence that one of these
137 four bases will stabilize clusters more than the others: they behave similarly during the 3 s
138 reaction time. In addition, the evaporation rates are interconnected in the complex series of
139 cluster balance equations. Different types of experiments, ones more sensitive to small
140 differences in slow evaporation rates, are required to better quantify evaporation, decomposition,
141 and partial chemical ionization rates.
142

Table S1 List of evaporation rates used for the model

Base	E_1 (s^{-1})	E_{2B} (s^{-1})	E_2 (s^{-1})	E_{3A3B} (s^{-1})	E_{3A3B2} (s^{-1})
DMA	0.1	0	0	1	1
EDA	5	0	0	0	0
Put	5	0	0	0	0
TMEDA	5	0	0	0	0

143

Table S2 Summary of all the reactions modeled in this study. Note, reactions are unbalanced and written in shorthand.

Neutral cluster formation	CI and ion decomposition reactions	IIC reactions
$A_1 + B \underset{E_1}{\overset{k}{\rightleftharpoons}} AB$	$A_2B_2 + NO_3^- \xrightarrow{k_c} A_2B_2^- \xrightarrow{fast} A_2^-$	$A_1^- + A_1 \xrightarrow{k_c} A_2^-$
$AB + A_1 \xrightarrow{k} A_2B$	$AB + NO_3^- \xrightarrow{k_c} AB^- \xrightarrow{fast} A_1^-$	$A_2^- + A_1$ or $AB \xrightarrow{k_c} A_3^-$
$AB + AB \xrightarrow{k} A_2B_2$	$A_1 + NO_3^- \xrightarrow{k_c} A_1^-$	$A_1^- + A_2B \xrightarrow{k_c} A_3B^-$
$A_2B + B \xrightarrow{k} A_2B_2$	$A_2B + NO_3^- \xrightarrow{k_c} A_2B^- \xrightarrow{fast} A_2^-$	$A_1^- + A_3B \xrightarrow{k_c} N_4^-$
$A_2B + A_1 \xrightarrow{k} A_3B$	$A_3B + NO_3^- \xrightarrow{k_c} A_3^-B \xrightarrow{E_{A3B^-}} A_2^- + A_1B$	$A_1^- + A_2B_2 \xrightarrow{k_c} A_3B_2^-$
$A_3B + B \xrightarrow{k} A_3B_2$	$N_4 + NO_3^- \xrightarrow{k_c} N_4^-$	$A_1^- + AB \xrightarrow{k_c} A_2B^- \xrightarrow{fast} A_2^-$
$A_2B_2 + A_1 \xrightarrow{k} A_3B_2$	$A_3B_3 + NO_3^- \xrightarrow{k_c} A_3^-B_3 \xrightarrow{fast} A_3^-B_2$	
$A_2B + AB \xrightarrow{k} A_3B_2$	$A_3B_2 + NO_3^- \xrightarrow{k_c} A_3B_2^- \xrightarrow{E_{A3B2^-}} A_3B^-$	
$A_2B_2 + AB \xrightarrow{k} A_3B_3$		
$A_3B_2 \xrightarrow{E_{A3B2}} A_2B_2 + A_1$		
A_3B or A_3B_2 or $A_3B_3 + AB \xrightarrow{k} N_4$		
A_3B_2 or $A_3B_3 + A_1 \xrightarrow{k} N_4$		
$A_2B_2 \xrightarrow{E_2} AB + AB$		
$A_2B_2 \xrightarrow{E_{2B}} A_2B + B$		
$A_3B \xrightarrow{E_{A3B}} A_2B + A_1$		

146	
147	References:
148	

149 Berresheim, H., Elste, T., Plass-Dülmer, C., Eisele, F. L., and Tanner, D. J.: Chemical ionization
150   mass spectrometer for long-term measurements of atmospheric OH and H_2SO_4, International
151   Journal of Mass Spectrometry, 202, 91-109, 10.1016/s1387-3806(00)00233-5, 2000.
152 Eisele, F. L., and Hanson, D. R.: First Measurement of Prenucleation Molecular Clusters, The
153   Journal of Physical Chemistry A, 104, 830-836, 10.1021/jp9930651, 2000.
154 Rosser, S., and de la Mora, J. F.: Vienna-Type DMA of High Resolution and High Flow Rate,
155   Aerosol Science and Technology, 39, 1191-1200, 10.1080/02786820500444820, 2005.
156 Ude, S., and de la Mora, J. F.: Molecular monodisperse mobility and mass standards from
157   electrosprays of tetra-alkyl ammonium halides, Journal of Aerosol Science, 36, 1224-1237,
158   10.1016/j.jaerosci.2005.02.009, 2005.
159 Zhao, J., Eisele, F. L., Titcombe, M., Kuang, C., and McMurry, P. H.: Chemical ionization mass
160   spectrometric measurements of atmospheric neutral clusters using the cluster-CIMS, J.
161   Geophys. Res., 115, D08205, 10.1029/2009jd012606, 2010.
162
163